Available online at www.sciencedirect.com
ScienceDirect
International Journal of Thermal Sciences 45 (2006) 1158–1165
International Journal of Thermal Sciences
www.elsevier.com/locate/ijts

Effect of fluid thermal properties on the heat transfer characteristics in a double-pipe helical heat exchanger

Timothy J. Rennie, Vijaya G.S. Raghavan *

Department of Bioresource Engineering, McGill University, 21 111 Lakeshore Rd., Sainte Anne-de-Bellevue, QC H9X 3V9, Canada

Received 15 September 2004; received in revised form 21 February 2005; accepted 20 February 2006

Available online 20 March 2006

Abstract

Heat transfer characteristics of a double-pipe helical heat exchanger were numerically studied to determine the effect of fluid thermal properties on the heat transfer. Two studies were performed; the first with three different Prandtl numbers (7.0, 12.8, and 70.3) and the second with thermally dependent thermal conductivities. Thermal conductivities of the fluid were based on a linear relationship with the fluid temperature. Six different fluid dependencies were modeled. Both parallel flow and counterflow configurations were used for the second study.

Results from the first study showed that the inner Nusselt number was dependent on the Prandtl number, with a greater dependency at lower Dean numbers; this was attributed to changing hydrodynamic and thermal entry lengths. Nusselt number correlations based on the Prandtl number and a modified Dean number are presented for the heat transfer in the annulus. Results from the second part of the study showed that the Nusselt number correlated better using a modified Dean number. The counterflow configuration had higher heat transfer rates than the parallel flow, but the ratio of these differences was not different when comparing thermally dependent properties and thermally independent properties.
© 2006 Elsevier Masson SAS. All rights reserved.

Keywords: Double-pipe; Heat exchanger; Dean number; Laminar flow; Prandtl number

1. Introduction

Using correct and proper values for fluid properties are important when designing a heat exchanger for a particular process, especially for the heating and cooling of complex fluids, such as food products. These properties are a factor in both the rate of heat transfer (and hence the required size of the heat exchanger) as well as the pressure drop across the heat exchanger, which is important for assuring correct pump selection. Temperature dependent properties complicate the design of heat exchangers for specific processes. The prediction of the developing hydrodynamic and thermal boundary layers can be quite complex and difficult. Numerical methods and/or experiments are often required.

Recently there has been significant investigation into the benefits of using helical heat exchangers in food processing applications [1–7], with one of the benefits being higher heat transfer coefficients compared to straight tube helical heat exchangers due to tube curvature [8,9]. The curvature results in secondary flow patterns, perpendicular to the main axial flow, which increase fluid mixing. A reduction in the residence time distribution is obtained with helical heat exchangers [3], which can be important in maximizing quality retention of processed foods.

For the most part, heat transfer characteristics for tube flow are described using dimensionless numbers, with the Nusselt number expressed as a function of the Reynolds number and the Prandtl number. However, for helical coils, the Reynolds number is often replaced by the Dean number [8,9], which is defined as the Reynolds number multiplied by the square root of the curvature ratio (the ratio of the radius of the tube to the radius of curvature). The Dean number is used to represent the strength of the secondary flows; however, not all correlations for heat transfer in helical coils utilize the Dean number [10]. Other correlations have been based on friction factors [11], the Graetz number (in the case of developing flow) [12], and/or the curvature ratio [13].

* Corresponding author. Tel.: +1 514 398 8731; fax: +1 514 398 8387.
E-mail address: vijaya.raghavan@mcgill.ca (G.S.V. Raghavan).

1290-0729/$ – see front matter © 2006 Elsevier Masson SAS. All rights reserved.
doi:10.1016/j.ijthermalsci.2006.02.004

Nomenclature

a	constant	
A	constant	$\mathrm{W\,m^{-1}\,K^{-1}}$
b	constant	
B	constant	$\mathrm{W\,m^{-1}\,K^{-2}}$
c	constant	
c_p	specific heat	$\mathrm{J\,kg^{-1}\,K^{-1}}$
d	diameter of inner tube	m
D_o	outer diameter of annulus	m
D_i	inner diameter of annulus	m
De	Dean number ($Re\sqrt{\frac{d}{2R}}$)	
De^*	modified Dean number for the annulus ($\frac{\rho V}{\mu}(D_o - D_i)(\frac{D_o - D_i}{R})^{1/2}$)	
$De^\dagger$	modified Dean number for the annulus ($\frac{\rho V}{\mu}(D_o - D_i)(\frac{D_o}{2R})^{1/2}$)	
Gz^*	modified Graetz number ($De^* Pr\frac{d}{x}$)	
$Gz^\dagger$	modified Graetz number ($De^\dagger Pr\frac{d}{x}$)	
h_i	inner heat transfer coefficient	$\mathrm{W\,m^{-2}\,K^{-1}}$
h_0	outer heat transfer coefficient	$\mathrm{W\,m^{-2}\,K^{-1}}$
k	thermal conductivity	$\mathrm{W\,m^{-1}\,K^{-1}}$
Nu_i	inner tube Nusselt number ($\frac{h_i d}{k}$)	
Nu_o	annulus Nusselt number ($\frac{h_o(D_o - D_i)}{k}$)	
Pr	Prandtl number ($\frac{\mu/\rho}{k/\rho c_p} = \frac{\mu c_p}{k}$)	
r	cylindrical-polar coordinate	m
R	radius of curvature	m
T	temperature	K
T_{abs}	absolute temperature	K
V	average velocity	$\mathrm{m\,s^{-1}}$
x	axial distance	m
z	cylindrical-polar coordinate	m
Greek symbols		
θ	cylindrical-polar coordinate	m
ρ	density	$\mathrm{kg\,m^{-3}}$
μ	viscosity	$\mathrm{kg\,m^{-1}\,s^{-1}}$

The majority of these cases are for thermal boundary conditions of constant wall temperature or constant wall flux, which are different from the boundary conditions found in a fluid-to-fluid heat exchanger [14]. Thermal boundary conditions can affect the Nusselt number; it is well known that for fully developed flow in straight pipes the Nusselt number differs based on the thermal boundary conditions. Under these conditions, changing the flow rate, fluid properties or fluid temperature on one side of the heat exchanger can affect the heat transfer and fluid flow characteristics on the other side of the heat exchanger. For example, increasing the flow rate tends to increase heat transfer rates, which result in an increase/decrease of the average temperature of the fluid on the other side of the barrier. Thus the fluid properties, such as thermal conductivity, density, and viscosity, may change. If the viscosity decreases, the average pressure drop will also decrease. Depending on the type of pump used, this could result in an increased flow rate. Thus it is important to investigate and understand the effects of thermally dependent fluid properties, and how flow rates and geometry can affect the heat transfer characteristics when dealing with thermally dependent properties, as often found in food processing applications.

2. Objective

The objective of this work is to study the effects of fluid thermal properties on the heat transfer characteristics for double-pipe helical heat exchangers. The work was performed using a computational fluid dynamics package (PHOENICS 3.3). The set goals were achieved in two stages:

(1) Determination of the effects of the Prandtl number;
(2) Determination of the effects of thermally dependent thermal conductivity.

3. Materials and methods

3.1. CFD modeling

Geometries for the heat exchanger were created in AutoCAD 14 and exported as stereolithography files. Three different coils were created, one for the annulus, with inner and outer diameters of 0.1 and 0.115 m, respectively, and with a pitch of 0.115 m. The two other coils were created with outer diameters of 0.04 and 0.06 m, both with a pitch of 0.115 m and with a wall thickness that was 15% of the respective outer diameters. Each of the coils had a length of 2π (one full turn).

The geometry files were imported into a computational fluid dynamics software (PHOENICS 3.3), which is based on a control volume-finite difference formulation. A schematic of the cross-sectional view of the heat exchangers, a long with the coordinate system, is shown in Fig. 1. A cylindrical-polar coordinate system (r–θ–z) was used with a mesh size of $30 \times 40 \times 80$ in the axial (θ), horizontal (r), and vertical directions (z), respectively. In cylindrical-polar coordinates (r–θ–z), the continuity equation, momentum equations, and energy equation, respectively, can be written as:

$$\frac{\partial \rho}{\partial t} + \frac{1}{r}\frac{\partial(\rho r v_r)}{\partial r} + \frac{1}{r}\frac{\partial(\rho v_\theta)}{\partial \theta} + \frac{\partial(\rho v_z)}{\partial z} = 0 \tag{1}$$

$$\begin{aligned}\frac{\partial v_r}{\partial t} + v_r\frac{\partial v_r}{\partial r} + \frac{v_\theta}{r}\frac{\partial v_r}{\partial \theta} + v_z\frac{\partial v_r}{\partial r} - \frac{v_\theta^2}{r} \\ = -\frac{1}{\rho}\frac{\partial p}{\partial r} + \frac{\mu}{\rho}\left(\frac{1}{r}\frac{\partial}{\partial r}\left(r\frac{\partial v_r}{\partial r}\right) + \frac{1}{r^2}\frac{\partial^2 v_r}{\partial \theta^2} + \frac{\partial^2 v_r}{\partial z^2} \right. \\ \left. - \frac{v_r}{r^2} - \frac{2}{r^2}\frac{\partial v_\theta}{\partial \theta}\right)\end{aligned} \tag{2}$$

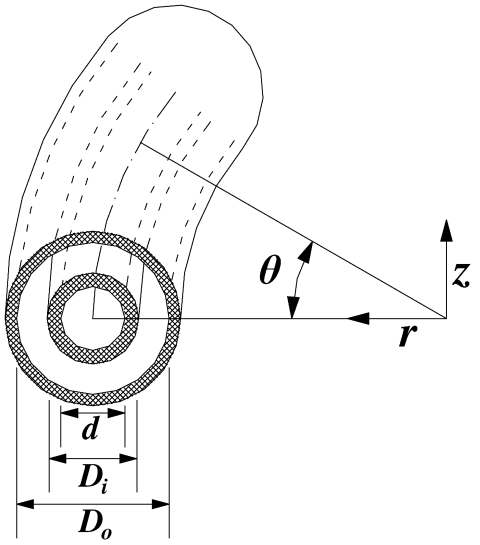

Fig. 1. Schematic of the geometry of heat exchanger and coordinate system.

$$\frac{\partial v_\theta}{\partial t} + v_r\frac{\partial v_\theta}{\partial r} + \frac{v_\theta}{r}\frac{\partial v_\theta}{\partial \theta} + v_z\frac{\partial v_\theta}{\partial r} + \frac{v_r v_\theta}{r} = -\frac{1}{\rho r}\frac{\partial p}{\partial \theta} + \frac{\mu}{\rho}\left(\frac{1}{r}\frac{\partial}{\partial r}\left(r\frac{\partial v_\theta}{\partial r}\right) + \frac{1}{r^2}\frac{\partial^2 v_\theta}{\partial \theta^2} + \frac{\partial^2 v_\theta}{\partial z^2} - \frac{v_\theta}{r^2} + \frac{2}{r^2}\frac{\partial v_r}{\partial \theta}\right) \tag{3}$$

$$\frac{\partial v_z}{\partial t} + v_r\frac{\partial v_z}{\partial r} + \frac{v_\theta}{r}\frac{\partial v_z}{\partial \theta} + v_z\frac{\partial v_z}{\partial r} = -\frac{1}{\rho}\frac{\partial p}{\partial z} + \frac{\mu}{\rho}\left(\frac{1}{r}\frac{\partial}{\partial r}\left(r\frac{\partial v_z}{\partial r}\right) + \frac{1}{r^2}\frac{\partial^2 v_z}{\partial \theta^2} + \frac{\partial^2 v_z}{\partial z^2}\right) \tag{4}$$

$$\rho c_p\left(\frac{\partial T}{\partial t} + v_r\frac{\partial T}{\partial r} + \frac{v_\theta}{r}\frac{\partial T}{\partial \theta} + v_z\frac{\partial T}{\partial z}\right) = k\left(\frac{\partial^2 T}{\partial r^2} + \frac{1}{r}\frac{\partial T}{\partial r} + \frac{1}{r^2}\frac{\partial^2 T}{\partial \theta^2} + \frac{\partial^2 T}{\partial z^2}\right) \tag{5}$$

The coils were orientated in a vertical position, though the results are also appropriate for horizontal coils as the buoyancy forces were not activated. However, the results from this study must be regarded with caution for fluids that experience significant changes in density due to temperature changes. The radius of curvature for all coils was 0.8 m. Inlets and outlets were located at each end of the coil. The boundary conditions associated with the inlets specified the inlet velocities in the axial direction. At all solid–fluid interfaces, the fluid velocities were set to zero, representing a no-slip condition. Coil properties were set to those of stainless steel, with a thermal conductivity of 16 $\mathrm{W\,m^{-1}\,K^{-1}}$, density of 7881.8 $\mathrm{kg\,m^{-3}}$ and a specific heat of 502 $\mathrm{J\,kg^{-1}\,K^{-1}}$. The outer coil was set to adiabatic conditions (representing an insulated tube) and the inner coil was set to allow conductive heat flow through the tube walls. The flow regime for all trials was in the laminar region and the fluid was treated as Newtonian. The model was tested by simulating heat transfer in a single helical coil with constant temperature and constant heat flux thermal boundary conditions. The results from these simulations were compared to published data [15]. The simulations were also compared to experimental data. The results of the experimental work are described in [16]. The literature and experimental data confirmed the validity of the numerical approach used in this study. Further details of the computational and experimental procedures can be found in Rennie and Raghavan [15,16].

3.2. Prandtl numbers

The Prandtl number is a dimensionless parameter that is a fluid property and is defined as the relative thickness of the hydrodynamic layer and the thermal boundary layer [17]. In the first set of simulations, the Prandtl number was varied using three different values, 7.03, 12.8, and 70.3. These different Prandtl numbers were achieved by changing the thermal conductivity of the fluid, using thermal conductivities of 0.597, 0.328, and 0.0597 $\mathrm{W\,m^{-1}\,K^{-1}}$, along with a dynamic viscosity of 1.004×10^{-3} $\mathrm{kg\,m^{-1}\,s^{-1}}$, and a heat capacity of 4181.8 $\mathrm{J\,kg^{-1}\,K^{-1}}$. Four different mass flow rates were used in the inner tube (0.00835, 0.02504, 0.04174 and 0.05843 $\mathrm{kg\,s^{-1}}$). For each of these flow rates, three simulations were performed, one with an annulus mass flow rate that has half the inner value, one with an equal value, and one that had double the inner mass flow rate, resulting in 12 different flow combinations. These combinations were performed using both coil sizes and the three Prandtl numbers resulting in a total of 72 trials.

3.3. Thermally dependent thermal conductivities

The second set of simulations focused on thermally dependent thermal conductivities. In this set, two different mass flow rates were used in the inner tube (0.00835 and 0.05843 $\mathrm{kg\,s^{-1}}$), with flow rates in the annulus which were either half or double the value in the inner tube, resulting in four different flow combinations. Six different model fluids were used. The thermal conductivities of these fluids were based on the following relationship:

$$k = A + BT_{\mathrm{abs}} \tag{6}$$

The specific heat, density, and dynamic viscosity of the fluid were constant with values of 4181.8 $\mathrm{J\,kg^{-1}\,K^{-1}}$, 998.23 $\mathrm{kg\,m^{-3}}$, and 1.004×10^{-3} $\mathrm{kg\,m^{-1}\,s^{-1}}$, respectively.

This results in a linear relationship between the thermal conductivity of the fluid and the absolute temperature, T_{abs}. The particular values used for the constants, A and B, are given in Table 1, along with the percent change the fluid undergoes if heated from 20 °C to 80 °C. Fluids K4, K5, and K6 were also tested in a counterflow configuration, using the four different flow combinations and the two different tube sizes.

Table 2 shows a selection [18] of some common food products along with the percent change of the thermal conductivity occurring between two temperatures. For the most part, these food products would have a relationship with temperature similar to fluid K2. Other thermal conductivity values have been added to adequately cover additional cases that could possibly occur in the food industry. Although these are in reference to the food industry, the analysis of the results is in dimensionless

Table 1
Constants used in Eq. (1) and percent change in thermal conductivity

Fluid	A [W m^{-1} K^{-1}]	B [W m^{-1} K^{-2}]	% change
K1	0.451	0.000498	5
K2	0.306	0.000995	10
K3	0.0139	0.00199	20
K4	−0.569	0.00398	40
K5	−1.444	0.00697	70
K6	−2.318	0.00995	100

Table 2
Thermal conductivities of select food products [18]

Food product	Temperature [°C]	Thermal conductivity [W m^{-1} K^{-1}]	% change
Apple juice, 80% H_2O	20	0.559	12.9
	80	0.631	
Grape juice, 89% H_2O	20	0.567	12.7
	80	0.639	
Whole milk	20	0.550	11.6
	80	0.614	
Sucrose solution, 40% H_2O	20	0.404	12.4
	80	0.454	
Glucose solution, 90% H_2O	20	0.566	12.9
	80	0.639	
Honey, 80% H_2O	2	0.502	−17.3
	69	0.415	

parameters and should prove useful for applications outside the food processing industry.

4. Results and discussion

4.1. Prandtl effects in the inner tube

Three different Prandtl numbers were used 7.0, 12.8, and 70.3. Each of these was achieved by adjusting the thermal conductivity of the fluid, while the other fluid properties (density, viscosity, and specific heat) were not changed. In this work, the difficulty to determine the appropriate effect of the Prandtl number is augmented by the developing hydrodynamic and thermal entrance regions. For each Dean number, the hydrodynamic entrance region is of different lengths, which also affects the thermal entrance region. Hence it is difficult to correlate the data to a simple power law equation, as the entrance effects can become large as the Prandtl number increases. However, there are 24 simulations that have corresponding simulations that only differ by the Prandtl numbers used. That is, for any given simulation, there are two other simulations that are operated under the same conditions, except for the Prandtl number. In order to determine the effect of the Prandtl number on the Nusselt number, the ratio of the Nusselt numbers (for any two simulations with the same operating parameters) were calculated. Two different ratios were used, each were based on the Nusselt number for a given Prandtl number (12.8 or 70.3) divided by the Nusselt number with the lowest Prandtl number (7.0). Fig. 2 shows a plot of the increase in Nusselt number versus the Dean number. The ratio of the Nusselt numbers tends

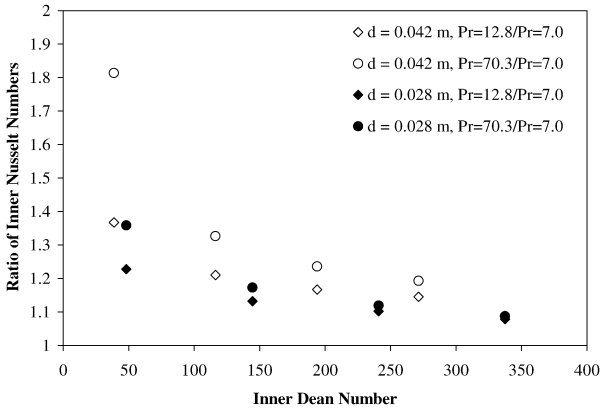

Fig. 2. Ratio of inner Nusselt number when the Prandtl number is changed from 7.0 to 12.8 or from 7.0 to 70.3, versus the inner Dean number.

to decrease with increasing Dean number, which could be attributed to the changing hydrodynamic entry length. For the most part, the effect of different Prandtl numbers on the Nusselt number is limited to low Dean numbers. However, this is not a general statement, as the hydrodynamic and thermal entrance regions are affected by the Dean number. Furthermore, the Prandtl number affects the developing thermal boundary layer, tending to increase the entry length as it is increased.

The effect of the Prandtl and Dean numbers on the Nusselt number is often presented as a power law equation, in the following form:

$$Nu = a\,De^{b}Pr^{c} \tag{7}$$

For any given set of flow conditions (flow rate, tube size) that only differs due to the Prandtl number, then the ratio of the Nusselt numbers can be expressed as:

$$\frac{Nu_2}{Nu_1} = \left(\frac{Pr_2}{Pr_1}\right)^{c} \tag{8}$$

The constant can be evaluated as follows:

$$c = \frac{\ln(Nu_2/Nu_1)}{\ln(Pr_2/Pr_1)} \tag{9}$$

The values of the constant are plotted against the Dean number in Fig. 3. There is a definite decrease in this constant as the Dean number is increased. Increasing the Dean number could result in larger entrance length. Generally, increasing the Reynolds number increases the entrance length, though the curvature effects this change. The value of the constant ranged from 0 to 0.55. For helical coils, the Prandtl number effect on the heat transfer is often related to the Nusselt number in a power law formulation, along with the Reynolds number or the Dean number. Seban and McLaughlin [11] found that for laminar flow the power is one-third. Dravid et al. [19], found a relationship with an exponent of 0.175, for Dean numbers in the range of 50 to 2000 and Prandtl numbers from 5 to 175. Kalb and Seader [9,20] found an exponent of 0.0108 for low Prandtl numbers (0.005 to 0.05) and a constant wall heat flux, whereas for Prandtl numbers in the range of 0.7 to 5 they reported exponents of either 0.1 or 0.2, for constant wall heat flux and constant wall temperatures, respectively. Janssen and Hoogendoorn [21] found that an exponent of 0.167 worked well in their

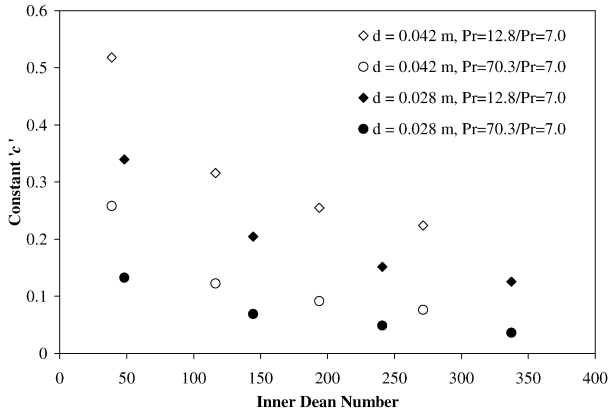

Fig. 3. Constant 'c' used in the inner Nusselt number correlations versus the inner Dean number. Plot shows when the Prandtl number is changed from 7.0 to 12.8 or from 7.0 to 70.3, with all other factors similar.

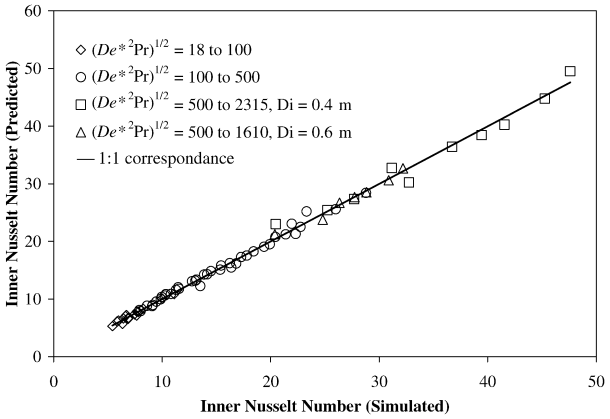

Fig. 4. Annulus Nusselt number predicted by Eqs. (10)–(13) compared to the numerically determined annulus Nusselt number.

correlations in the fully developed thermal region, whereas the Nusselt number was proportional to the Prandtl number to the power of 0.333 in the thermal entry region. The work present here differs slightly from the literature due to the boundary conditions and the pitch of the coil, which are usually not found in the literature, though they are conditions that are present in a double-pipe helical heat exchanger. The results suggest that the effect of the Prandtl number is lower as the Dean number increases. This could be due to increased mixing of the fluid by the secondary flow, and effectively decreasing the effect of the boundary layers on the heat transfer.

4.2. Prandtl effects in the annulus

Nusselt numbers were calculated for the annulus. These, unlike the flow in the inner tube, were less affected by entry effects. However, correlating the Nusselt number to the Prandtl and Dean numbers was limited to different ranges of $(De^{*2}Pr)^{1/2}$. This is not unusual, as other authors have often used different correlations depending on the range of one or more of the variables. Janssen and Hoogendoorn [21] used the variable $(De^2Pr)^{1/2}$ to describe ranges where certain correlations were applicable for flow in a helical coil. There does not appear to be any physical significance for this particular formulation. A similar approach was used in this study and three distinct regions were observed in this study. The highest range (with $(De^{*2}Pr)^{1/2}$ above 500) were divided into two correlations, one for each pipe size, as they could not be correlated together. The following correlations were developed in this work:

$$Nu = 2.08De^{*0.20}Pr^{0.28} \quad \text{for } 18 < \left(De^{*2}Pr\right)^{1/2} < 100, \quad R^2 = 0.955 \tag{10}$$

$$Nu = 0.39De^{*0.58}Pr^{0.46} \quad \text{for } 100 < \left(De^{*2}Pr\right)^{1/2} < 500, \quad R^2 = 0.989 \tag{11}$$

$$Nu = 2.70De^{*0.30}Pr^{0.29} \quad \text{for } 500 < \left(De^{*2}Pr\right)^{1/2} < 2315,\ d = 0.4, \quad R^2 = 0.969 \tag{12}$$

$$Nu = 5.27De^{*0.20}Pr^{0.19} \quad \text{for } 500 < \left(De^{*2}Pr\right)^{1/2} < 1610,\ d = 0.6, \quad R^2 = 0.974 \tag{13}$$

For these ranges, the number of data points used was 16, 39, 10, and 7, respectively. The predicted values (from each corresponding equation) versus the simulated values for the Nusselt numbers are presented in Fig. 4. The square of the correlation coefficient for all the correlations was close to unity. The Dean number used in these correlations is a modified Dean number for the curved annulus:

$$De^* = \frac{\rho V}{\mu}(D_o - D_i)\left(\frac{D_o - D_i}{R}\right)^{1/2} \tag{14}$$

4.3. Thermally dependent thermal conductivity

In most calculations for heat transfer coefficients the fluid properties are assumed to be constant and taken at the mean temperature of the fluid. Even for basic systems this can pose a problem. If the outlet temperature is not known, then an iterative procedure is required to calculate the heat transfer coefficient and the temperature drop. This is further complicated if there are two fluids (such as a fluid-to-fluid heat exchanger) and if the fluid properties change with temperature. If the fluid properties are constant, then changing the flow properties on one side of the tube wall should not affect the Nusselt number on the other side of the tube wall for fully developed flow. However, this is not so if the fluid properties are temperature dependent. The effects of changing the flow rate in the annulus on the Nusselt number in the inner tube is shown in Fig. 5. Here, the original Nusselt number is shown on the x-axis, and the percent increase in the Nusselt number is shown on the y-axis when the flow in the annulus is increased fourfold. The data is broken up into 4 sections, one for each of the inner Reynolds numbers. The trials with the lower Reynolds numbers were affected more by the change than the trials with the larger Reynolds number.

Increased flow rate in the annulus results in a larger temperature gradient for heat transfer. These increased temperature gradients result in higher heat transfer rates, which allow the inner fluid to cool down quicker, resulting in lower thermal conductivities in the fluid. This effectively increases the average

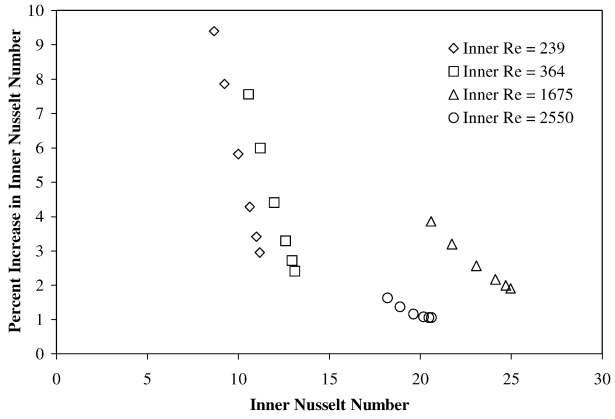

Fig. 5. Percent increase of the inner Nusselt number when the flow rate in the annulus was increased fourfold. Four inner Reynolds numbers were studied.

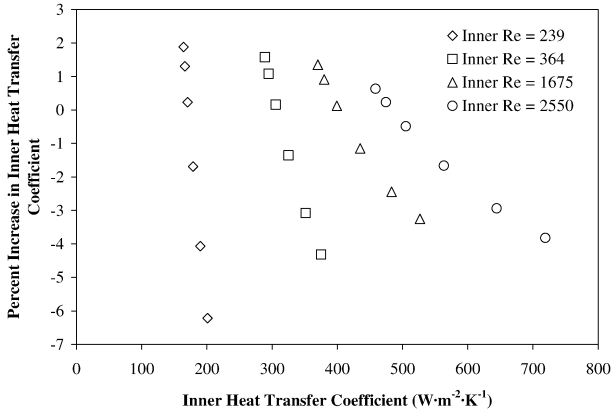

Fig. 6. Percent increase of the inner heat transfer coefficient when the flow rate in the annulus was increased fourfold. Four inner Reynolds numbers were studied.

Prandtl number (relative thickness of hydrodynamic and thermal boundary layers), and increases the Nusselt number. However, unlike the case of constant fluid properties, an increase in the Nusselt number for fluids with thermally dependent conductivities does not necessarily mean an increase in heat transfer coefficients. Recall that the Nusselt number is the ratio of the heat transfer coefficient (multiplied by a characteristic length) divided by the thermal conductivity. Thus the change may be due to a change in the thermal conductivity rather than the heat transfer coefficient. Fig. 6 shows the percent increase in the inner heat transfer coefficient versus the inner heat transfer coefficient for the 4 different Reynolds numbers when the flow in the annulus is increased fourfold. It can be seen here that the increase in the heat transfer coefficient can be negative or positive, depending on the strength of the thermal dependence. The highest percent increases are for fluid K1, which has the least thermal dependency of all the fluids. With increasing thermal dependency (K1 to K6), the increase in heat transfer coefficient is less.

The difficulty in determining the exact effect of the thermally dependent thermal conductivity on the heat transfer coefficients is complicated due to the fact that both fluids (in the inner tube and in the annulus) use a thermally dependent thermal conductivity. It would have been ideal to have one of them constant

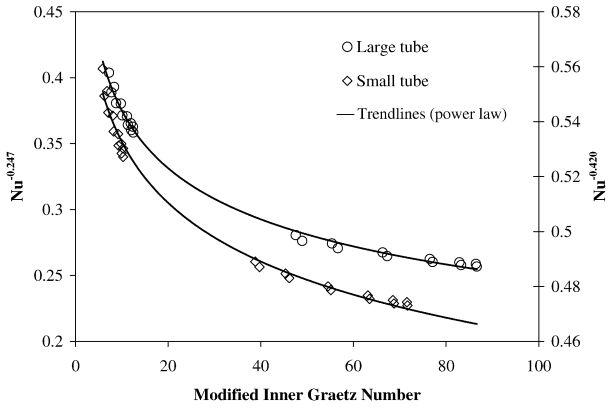

Fig. 7. Inner Nusselt number to the exponent −0.247 (small tube) and to the exponent −0.420 (large tube) versus the modified inner Graetz number.

(no temperature effect). This would keep one of the entry regions constant, and the analysis could focus only on the tube that had the thermally dependent thermal conductivity. However, the inner Nusselt numbers can be correlated to a modified Graetz number, Gz^*:

$$Gz^* = De^* Pr \frac{d}{x} \tag{15}$$

where d is the diameter of the inner tube and x is the axial distance along the tube. The Reynolds number, which is usually present in the Graetz number, has been replaced with the Dean number. Two different correlations were performed, one for each of the tube sizes. The results are presented in Fig. 7. The two correlation equations are:

$$Nu = 7.31 Gz^{*0.247} \quad \text{for } d = 0.28 \text{ m}, \quad R^2 = 0.994 \tag{16}$$

$$Nu = 3.94 Gz^{*0.420} \quad \text{for } d = 0.42 \text{ m}, \quad R^2 = 0.996 \tag{17}$$

The same procedure was used to determine the Nusselt number in the annulus, but the Dean number used in the modified Graetz number was calculated with the following equation, rather than Eq. (9):

$$De^\dagger = \frac{\rho V}{\mu}(D_o - D_i)\left(\frac{D_o}{2R}\right)^{1/2} \tag{18}$$

The only difference between Eqs. (14) and (18) is the expression used for the curvature ratio. The expression in Eq. (14) takes into consideration the gap distance of the annulus, whereas Eq. (18) simply uses the outer diameter of the annulus and the radius of curvature. It was found that the formulation used in Eq. (18) correlated the results better for this section. The correlation equation developed was as follows:

$$Nu = 0.173 Gz^\dagger + 5.75, \quad R^2 = 0.978 \tag{19}$$

The correlation is shown in Fig. 8. This correlation gives an asymptotic Nusselt number of 5.75, whereas in Rennie and Raghavan [15], the asymptotic Nusselt number (for the Dean–Nusselt correlation) gave an asymptotic value of 5.36. However, the correlation in Rennie and Raghavan [15] did not take into consideration thermally dependent thermal conductivities of the fluid.

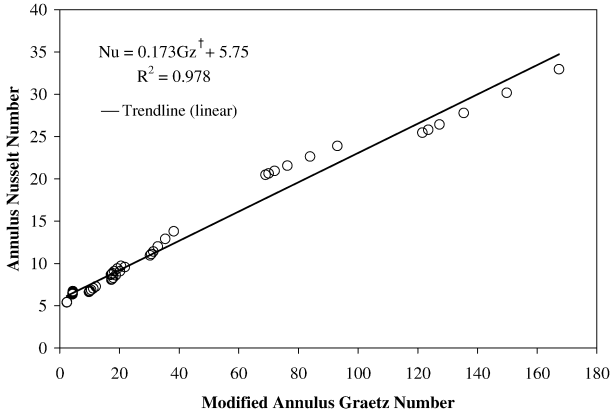

Fig. 8. Annulus Nusselt number versus the modified annulus Graetz number.

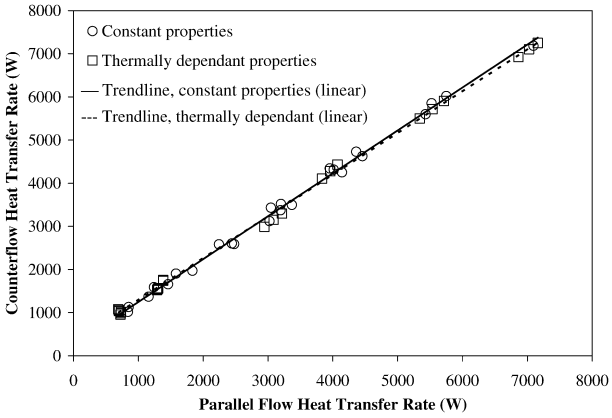

Fig. 9. Counterflow heat transfer rate versus parallel flow heat transfer rate for either constant properties or thermally dependant properties.

Parallel flow versus counterflow heat exchangers were compared to determine the effects thermal dependent conductivities had on the heat transfer rates. The first, and obvious effect, is due to the nature of counterflow heat exchangers, they result in larger heat transfer rates, and hence larger temperature changes. This results in changes to the Graetz number in both the inner and the outer annulus (due to changes in average Prandtl number). However, with the two fluids having the same thermal dependence, one drops in average Prandtl number, while the other experiences an increase in the average Prandtl number. This situation exists for parallel flow and counterflow configurations. However, in a parallel flow heat exchanger, along the length of the heat exchanger, one fluid has an increasing thermal conductivity while the other has a decreasing thermal conductivity. Therefore, the thermal resistance will decrease on one side of the tube, and the resistance will increase on the other side, partially canceling each other out in the overall effect. For a counterflow heat exchanger, the highest thermal resistances will both be located at one end of the heat exchanger (at the cold inlet and hot outlet) and the lowest thermal resistances at the other end. This results in two very different distributions of thermal resistances, as well as temperature profiles. Fig. 9 shows the heat transfer rates of counterflow versus parallel flow for both thermally stable and thermally dependent fluid thermal conductivities. The ratio between the two heat transfer rates is not affected by the changing thermal properties. Though the properties do change more in a counterflow configuration, due to the large temperature changes, they did not have any additional effects.

5. Conclusions

A computational fluid dynamics package (PHOENICS 3.3) was used to numerically study the effects of fluid thermal properties on the heat transfer characteristics in a double-pipe helical heat exchanger. Three levels of Prandtl numbers were used; these were modified by changing the thermal conductivity. The Nusselt number was shown to be much more sensitive to changes in the Prandtl number at low Dean numbers than at higher Dean numbers. These changes were attributed to changes in the developing thermal and hydrodynamic boundary layers. The Nusselt number in the annulus was correlated as a function of a modified Dean number and the Prandtl number. However, regions of $(De^{*2}Pr)^{1/2}$ were identified where multiple correlations were needed to adequately describe the relationship.

Thermally dependent thermal conductivities were studied using six different degrees of dependence. The results indicated that there can be significant changes in the Nusselt number based on the thermal dependency. Changing the flow rate in one tube can change the average thermal conductivity value to a fairly large degree, as well as changing the entry length for the developing thermal boundary layer. For both the inner tube and for the annulus, the Nusselt number correlated well with the Graetz number. The Graetz number used in this work, however, was not the standard Graetz number. It was modified by replacing the Reynolds number in the Graetz number calculation with the Dean number, for both the inner tube and the annulus. Though this worked well for the annulus, two different correlations were needed for the inner tube, one for each of the tube diameters, showing that further investigation needs to be made in this area.

Parallel flow versus countercurrent flow was studied to determine if the thermally dependent properties had any effect on the heat transfer rates. In counterflow conditions, greater heat transfer rates resulted in larger changes in fluid properties. When the ratio of the heat transfer rates for parallel flow versus counterflow were plotted against each other, there was no difference based on thermally dependent versus thermally stable fluid properties. This suggests that the location of the two developing flows is not relevant in the design of the heat exchanger. They can either be at the same end of the heat exchanger or at opposite ends, for the conditions observed in this study.

Acknowledgements

The authors are grateful to FCAR (Fonds pour la Formation de Chercheurs et l'Aide à la Recherche) and NSERC (Natural Sciences and Engineering Research Council of Canada) for the financial assistance for this study.

References

[1] K.P. Sandeep, C.A. Zuritz, V.M. Puri, Residence time distribution of particles during two-phase non-Newtonian flow in conventional as compared with helical holding tubes, J. Food Sci. 62 (4) (1997) 647–652.

[2] S. Grabowski, H.S. Ramaswamy, Bend-effects on the residence time distribution of solid food particles in a holding tube, Canad. Agr. Engrg. 40 (2) (1998) 121–126.

[3] J.D.H. Kelder, K.J. Ptasinski, P.J.A.M. Kerkhof, Power-law foods in continuous coiled sterilizers, Chem. Engrg. Sci. 57 (2002) 4605–4615.

[4] T.K. Palazoglu, K.P. Sandeep, Effect of holding tube configuration on the residence time distribution of multiple particles in helical tube flow, J. Food Process Engrg. 25 (2002) 337–350.

[5] P.K. Sahoo, Md.I.A. Ansari, A.K. Datta, Computer-aided design and performance of an indirect type helical tube ultra-high temperature (UHT) milk sterilizer, J. Food Engrg. 51 (2002) 13–19.

[6] P.K. Sahoo, Md.I.A. Ansari, A.K. Datta, A computer based iterative solution for accurate estimation of heat transfer coefficients in a helical tube heat exchanger, J. Food Engrg. 58 (2003) 211–214.

[7] J.D.H. Kelder, K.J. Ptasinski, P.J.A.M. Kerkhof, Starch gelatinization in coiled heaters, Biotechnol. Prog. 20 (2004) 921–929.

[8] Y. Mori, W. Nakayama, Study on forced convective heat transfer in curved pipes (1st report, laminar region), Int. J. Heat Mass Transfer 8 (1965) 67–82.

[9] C.E. Kalb, J.D. Seader, Heat and mass transfer phenomena for viscous flow in curved circular tubes, Int. J. Heat Mass Transfer 15 (1972) 801–817.

[10] B. Bai, L. Guo, Z. Feng, X. Chen, Turbulent heat transfer in a horizontally coiled tube, Heat Transfer Asian Res. 28 (5) (1999) 395–403.

[11] R.A. Seban, E.F. McLaughlin, Heat transfer in tube coils with laminar and turbulent flow, Int. J. Heat Mass Transfer 6 (1963) 387–395.

[12] V. Kubair, N.R. Kuloor, Heat transfer to Newtonian fluids in coiled pipes in laminar flow, Int. J. Heat Mass Transfer 9 (1966) 63–75.

[13] M.N. Ozisik, H.C. Topakoglu, Heat transfer for laminar flow in a curved pipe, J. Heat Transfer 90 (1968) 313–318.

[14] D.G. Prabhanjan, T.J. Rennie, G.S.V. Raghavan, Natural convection heat transfer from helical coiled tubes, Int. J. Thermal Sci. 43 (2004) 359–365.

[15] T.J. Rennie, G.S.V. Raghavan, Numerical studies of a double-pipe helical heat exchanger, App. Thermal Engrg. 26 (11–12) (2006) 1266–1273.

[16] T.J. Rennie, G.S.V. Raghavan, Experimental studies of a double-pipe helical heat exchanger, Exp. Thermal Fluid Sci. 29 (2005) 919–924.

[17] C.J. Geankoplis, Transport Processes and Unit Operations, Allyn and Bacon, Boston, MA, 1983.

[18] ASHRAE, Thermal properties of foods, in: Refrigeration Handbook, American Society of Heating, Refrigeration and Air-Conditioning Engineers, Atlanta, GA, 1998.

[19] A.N. Dravid, K.A. Smith, E.W. Merril, P.L.T. Brian, Effect of Secondary fluid motion on laminar flow heat transfer in helically coiled tubes, AIChE J. 17 (5) (1971) 1114–1122.

[20] C.E. Kalb, J.D. Seader, Fully developed viscous-flow heat transfer in curved circular tubes with uniform wall temperature, AIChE J. 20 (2) (1974) 340–346.

[21] L.A.M. Janssen, C.J. Hoogendoorn, Laminar convective heat transfer in helical coiled tubes, Int. J. Heat Mass Transfer 21 (1978) 1197–1206.